Computational and Structural Biotechnology Journal 21 (2023) 1349–1361

Contents lists available at ScienceDirect

Computational and Structural Biotechnology Journal

journal homepage: www.elsevier.com/locate/csbj

Electro-detachment of kinesin motor domain from microtubule in silico

Jiří Průša, Michal Cifra *

Institute of Photonics and Electronics of the Czech Academy of Sciences, Prague 18200, Czechia

ARTICLE INFO

Article history:
Received 27 August 2022
Received in revised form 15 January 2023
Accepted 15 January 2023
Available online 21 January 2023

Keywords:
Electric field
Proteins
Tubulin
Microtubules
Molecular dynamics simulation

ABSTRACT

Kinesin is a motor protein essential in cellular functions, such as intracellular transport and cell-division, as well as for enabling nanoscopic transport in bio-nanotechnology. Therefore, for effective control of function for nanotechnological applications, it is important to be able to modify the function of kinesin. To circumvent the limitations of chemical modifications, here we identify another potential approach for kinesin control: the use of electric forces. Using full-atom molecular dynamics simulations (247,358 atoms, total time ~ 4.4 μs), we demonstrate, for the first time, that the kinesin-1 motor domain can be detached from a microtubule by an intense electric field within the nanosecond timescale. We show that this effect is field-direction dependent and field-strength dependent. A detailed analysis of the electric forces and the work carried out by electric field acting on the microtubule–kinesin system shows that it is the combined action of the electric field pulling on the β-tubulin C-terminus and the electric-field-induced torque on the kinesin dipole moment that causes kinesin detachment from the microtubule. It is shown, for the first time in a mechanistic manner, that an electric field can dramatically affect molecular interactions in a heterologous functional protein assembly. Our results contribute to understanding of electromagnetic field–biomatter interactions on a molecular level, with potential biomedical and bio-nanotechnological applications for harnessing control of protein nanomotors.

1. Introduction

Molecular motor proteins, such as microtubule-associated kinesins, can be considered as highly evolved nanoscopic biological machines that have been perfected over billions of years of evolution. Kinesins are a superfamily of motor proteins with a diversity in structure and function [1]. Kinesin plays a key role in many cellular processes, from cell division to intracellular transport. In cell division, kinesins enable the generation of forces leading to spindle pole separation, spindle bipolarity and organization, chromosome positioning and congression [2,3]. Furthermore, kinesin is crucial for the transport of subcellular cargo such as vesicles and organelles. For example, it can transport synaptic vesicles from the cell body to the axon terminals in neurons, thus ensuring that neurotransmitters and neuroreceptors are transported to the correct locations [4]. Overall, kinesin is an essential motor protein involved in many cellular processes, from mitosis to the transport of proteins and other cargo. Without kinesin, these processes would be impossible. There are two major and complementary approaches for exploring the role and function of kinesin:in vitro and in in vivo. The in vitro approach typically relies on reconstituting the motor protein outside the cell in a well-controlled environment and provides a clearer interpretation between the structure and function of the motor protein. Such studies usually employ microscopy and molecular force measurement and enable, for example, understanding of the ATPase activity of kinesin and the kinesin stepping mechanism [5]. The in vivo (in cells and in organisms) approach enables researchers to observe the kinesin behavior in its native environment. Targeted (in cell and animal models) or natural (in humans and animals) mutations, allow the correlation of structural changes in kinesin to functional and patho/physiological changes in organism. For example, the dysfunction of kinesin is associated with diseases such as cancer [6] and neuropathies, mental impairment, and parkinsonism. [7,8]. In bionanotechnology, kinesin is a highly attractive nanomotor and has been used for nanoscale force generation [9], cargo shuttling [10], biomolecule sorting by charge [11], and parallel computation [12] Therefore, both in biomedicine and bionanotechnology, it is important to be able to modify the function of kinesin. To serve various tasks for nanotechnology purposes, a new motor has to be designed and produced, which is expensive and cumbersome. To circumvent the design and production of a new nanomotor to achieve a different function, we propose that an external intense

* Corresponding author.
E-mail address: cifra@ufe.cz (M. Cifra).

https://doi.org/10.1016/j.csbj.2023.01.018

pulsed electric field could be used to modify the kinesin–microtubule interaction, hence affecting and potentially controlling the kinesin function. There are two main lines of argument that support this proposal. First, electrostatic interactions are crucial for protein function [13–15] and protein-protein interactions [16,17] and kinesin itself was termed an electric machine [18]. Second, there is solid evidence that an electric field (EF) can affect protein structure [19] resulting in a change of protein function [20]. The prominent computational molecular dynamics simulation examples comprise protein rotation [21], change of the secondary structure [22] or dissociation of polymeric protein complexes [23], unfolding [24] and many more [25]. Experiments have confirmed that protein secondary structure can be affected by an EF [26] and, furthermore, have shown that EF can affect protein enzymatic function [20,26,27], self-assembly ability [28] or cause dissociation of protein aggregates [29].

Although there are several experimental [28,30–32] and theoretical works [21,23,33] demonstrating, for example, that an EF can affect the structure of tubulin and microtubules (MTs) [23] and can be used to steer MTs in kinesin gliding assays [11], little is known about the direct effect of an external EF on kinesin itself. Molecular dynamics simulations, in which EF and mechanical pull were combined, have shown that an intense oscillating EF (up to 10 GHz) affects (mostly decreases) the affinity of kinesin toward tubulin [34,35]. In our recent preliminary work [36], we demonstrated that under the influence of a static EF with a duration of several tens of nanoseconds, the kinesin dipole and contact surface area with the tubulin dimer were affected. However, until now, no major effect of EF has been observed on the interaction between kinesin and its microtubule track.

In this paper, we focus on kinesin-1, the first reported and one of the most explored kinesin families, which is known to play a role in a vesicle, organelle and mRNA transport [2]. The complete kinesin-1 is a heterotetramer consisting of two kinesin heavy chain and two kinesin light chain subunits [37]. However, there is evidence that a heavy chain kinesin subunit itself can act functionally in the absence of the light chain subunit, for example in the transport of mRNA granules [38], mitochondrial transport [39], cytoplasmic streaming [40], and microtubule–microtubule sliding [41]. In this work, we focus on the N-terminal motor domain of one of the kinesin heavy-chain subunits, since it is a force-producing subunit in a kinesin stepping process powered by ATP hydrolysis.

We uncovered qualitative new effects of EF on the kinesin–tubulin interaction of major importance, which have not been observed earlier. We first show that an external EF can detach a single kinesin motor domain from the microtubule. Then we clarify, in a quantified manner, the dependence of this effect on the EF direction, field strength and on coupling to the dipole and charge of the kinesin motor domain and β-tubulin C-terminus tail. Our results will inspire experimental work and open new avenues for electromagnetic modulation of biological and artificial active matter through action on noncovalent molecular interactions.

2. Methods

2.1. Molecular system and molecular dynamics simulations

Our molecular system (Fig. 1) is comprised of three tubulin heterodimers (from neighboring protofilaments of B-lattice microtubule and not neighboring the seam) [23] with a docked ADP-kinesin-1 motor domain (kinesin, in short). See the full structure topology files (.tpr gromacs file) in https://doi.org/10.48700/datst.3q9we-bks74.

Our kinesin corresponds to the kinesin-1 type (kif5b gene https://www.ncbi.nlm.nih.gov/gene/3799- present in variety of organisms including humans) and its structure is identical to that in [36,42] i.e., the kinesin model was built on the basis of an ADP-bound kinesin-1 structure (PDB ID: 1BG2, with neck linker truncated at residue 325), see details in [42]. The selection of this kinesin, which typically operates in a dimeric form, was motivated by our experimentally available kinesin constructs. For a detailed description of the MD simulation setup please see our associated Data in Brief paper.

Three tubulin heterodimers have a curvature corresponding to that as being in the microtubule wall [23]. The structure of the tubulin is available in the full structure topology files (.tpr gromacs file) in https://doi.org/10.48700/datst.3q9we-bks74. The tubulin structure is identical to that in [23], i.e., it contains GTP and originates from PDB structure ID 3J6E, see [43] for details.

In the simulation production run, all heavy atoms of the two outer heterodimers are kept in place by harmonic potential with the force constant 1000 kJ mol^{-1} nm^{-2} to represent the fact that the tubulin is bound in the microtubule lattice. The C-terminus of tubulin mentioned in all the quantitative analyses is defined as the chain of all residues from residue 403 to the end of the β-tubulin sequence.

Total number of atoms in simulations was 247,358 (For details see Table 1).

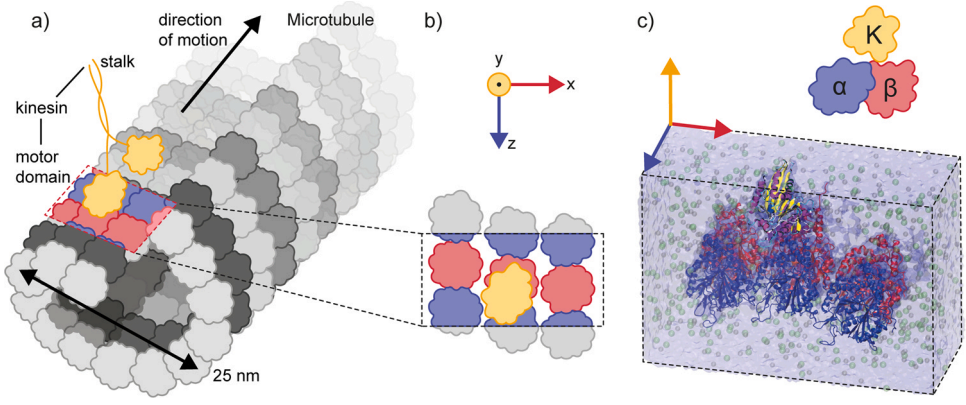

Fig. 1. The molecular system analyzed in this paper: a kinesin motor domain on a segment of a microtubule. a) A picture of the whole kinesin heavy chain nanomotor (yellow), which is a dimeric protein, bound to a microtubule (α and β tubulin in light and dark gray, respectively). Kinesin executes a stepping motion along the direction towards β-tubulin end of MTs, also called as plus end, it is -Z direction in the coordinates in this paper. b) Cartesian coordinates with a schematic of the segment which represents our system: three tubulin heterodimers with a single motor domain (head) of kinesin, periodically repeated to represent a microtubule (α and β tubulin in blue and red, respectively). c) snapshot of our system from a molecular dynamics simulation including the water box and ions.

Table 1
Molecular and atomic content of the simulated system.

–	molecules	number of atoms
Water (TIP3P)	66,653	199,959
K+	456	456
Cl-	300	300
α-tubulin	3	20,739 (6913 × 3)
β-tubulin	3	20,526 (6842 × 3)
Kinesin	1	5068
ADP	1	39
GTP	6	264 (44 × 6)
Mg2 +	7	7
Total	–	247,358

The EF was applied to the molecular system through a force $\vec{F_i}$ acting on each charged atom i in a simulation box: $\vec{F_i} = q_i\vec{E}$, where q_i is the charge of that atom and $\vec{E}$ is the vector of the electric field.

We obtained 40, 10, 10, 10 trajectories for 100 MV/m EF strength in the X, -X, Z, -Z EF directions, respectively. Additionally, we obtained 30, 20, 10 trajectories for 75 MV/m, 50 MV/m, 30 MV/m, respectively, for the X direction of EF. We did not explore lower field strengths, as the simulations required to observe the key effects, which we observe for the selected EF strength values, would be impractically long. The total simulation time was ~ 4.4 μs.

Additionally, we also ran a simulation in a big simulation box (see details in the associated Data in Brief paper), which was used for the potential of mean force analysis.

2.2. Analyses

2.2.1. Dipole moment of kinesin, dipole moment of β-tubulin C-terminus

The dipole moment was calculated using eq. (1).

$$\vec{p} = \sum_i^N q_i \vec{r_i}, \tag{1}$$

where q_i is the charge of atom i, $\vec{r_i}$ is its position vector with respect to kinesin (or β-tubulin C-terminus) center of mass and N total number of atoms in kinesin (or β-tubulin C-terminus).

2.2.2. Angle of kinesin, angle of β-tubulin C-terminus

We calculated the angle α between the dipole moment of kinesin (or β-tubulin C-terminus) $\vec{p}$ and vector pointing in the direction of the applied EF as:

$$\alpha = \arccos\frac{p_x}{|\vec{p}|}, \quad \text{for EF in X and -X direction} \tag{2}$$

and

$$\alpha = \arccos\frac{p_z}{|\vec{p}|}, \quad \text{for EF in Z and -Z direction} \tag{3}$$

where p_x and p_z are dipole components in x and z direction, respectively.

2.2.3. Number of contacts

The number of contacts between the kinesin and tubulin served as a metric to define a moment of kinesin detachment from the tubulin: the time when the number of contacts reached zero. For the analysis of the number of contacts, we first selected a subset of tubulin (alpha or beta) atoms that lie within a distance of 11 Å, from kinesin in the first frame, where we start to apply the EF. The distance of 11 Å corresponds to the cut-off of van der Waals interactions in our simulations. We excluded part of the C-terminus (residues number > 427) of β-tubulin from this subset, because the unstructured part of the β-tubulin C-terminus often sticks to the kinesin and follows it, even though the interaction energy between the kinesin and tubulin is practically at zero. This approach is justified by our energetics calculations (Fig. SI 1–13), which show that when the interaction energy reaches a plateau (corresponding to zero interaction), the distance of the kinesin displacement corresponds to distances when zero contacts are observed (as calculated by our approach). Then, for each frame from the trajectory, we took the number of kinesin atoms residing within this cut-off distance of 11 Å, from the original set of tubulin atoms as the number of contacts.

2.2.4. Distance of kinesin displacement and distance between kinesin and tubulin

The distance of kinesin displacement is the distance between the center of gravity between kinesin at frame 0 and kinesin at frame t. The kinesin–tubulin XY distance is the XY distance component between the center of gravity of the three tubulin heterodimers and kinesin at time t. Note that in trajectories with an EF in the X direction, the two quantities are approximately related to each other with an offset; e.g., a kinesin displacement of 2 nm (20 Å) corresponds to a kinesin–tubulin XY distance of approximately 7 nm.

2.2.5. Solvent accessible surface area - SASA

The solvent accessible surface area for central β-tubulin (excluding C-terminus tail) was obtained with the VMD built-in feature "measure sasa" with atom radii inherited from CHARMM36 forcefield.

2.2.6. Root-mean square displacement - RMSD

We measure the RMSD (as traditionally defined) by using the built-in VMD plugin RMSD. RMSD is evaluated for kinesin at frame 0 and frame t (fig. SI 1–8) and also per each kinesin residue (SI 1–9, SI 1–10).

2.2.7. Potential of mean force

We calculated the potential of mean force along the pathway of kinesin dissociation caused by the EF in the X direction in the big box with the weighted histogram analysis method (WHAM), as implemented [44] in GROMACS software package. We sampled the center of mass (COM) XY distance between kinesin and tubulins (allowing the Z dimension to move freely) in the range from ~ 5–10 nm with 27 separate windows. Each window was sampled with 15 ns MD simulation with restrained XY COM distance by umbrella (harmonic) potential with a depth of 500 kJ mol^{-1} nm^{-2}.

2.2.8. Force and work

The force acting on a molecule can be expressed from multipole expansion of the EF:

$$\vec{F} = q\vec{E} + \vec{p}\cdot(\nabla\vec{E}) + \frac{1}{2}\overleftrightarrow{\Theta}\cdot(\nabla\nabla\vec{E}) + \cdots \tag{4}$$

where $\overleftrightarrow{\Theta}$ is quadrupole moment of molecule.

And the work performed by the field:

$$W = \phi\vec{E} + \vec{p}\cdot\vec{E} + \frac{1}{2}\overleftrightarrow{\Theta}\cdot(\nabla\vec{E}) + \cdots \tag{5}$$

where ϕ stands for EF potential. Because we applied only a static (time) and homogeneous (space) external EF, we evaluated the work done by the field only from the two first terms in equation (5). The first term represents a translation (linear motion) work of the EF on a molecule. The translation work carried out in frame t was calculated as a product of the force acting on the sum charge of a molecule (kinesin and or β-tubulin C-terminus) displacement vector of the geometric center of molecule $\vec{d}$ during period $t-1$ to t.

$$W_{t,\mathrm{trans}} = \left(\sum_{i}^{kin} q_i\right)\vec{E}\cdot\vec{d} \tag{6}$$

The second is the work done by the field on dipole moment (rotational work) at frame t was calculated as:

$$W_{t,\mathrm{rot}} = \vec{E}\cdot d\vec{p} \tag{7}$$

3. Results and discussion

3.1. Detachment of kinesin is EF direction-dependent

First, we asked the question if the direction of the EF has any effect on the kinesin–tubulin interaction (for brevity, under *kinesin*, we refer to the kinesin-1 motor domain in all further text). Our earlier work suggested [36] that an EF acting parallel to kinesin–tubulin heterodimer (K-T) connection axis (direction Y and -Y in this paper) has a small effect on K-T interaction, in contrast to the EF perpendicular to the K-T connection axis. Therefore, in this paper, we focused on all four EF directions (100 MV/m field strength) that are perpendicular to the K-T connection axis, i.e., X,-X, Z, -Z and included the tubulin heterodimers from neighboring protofilaments (see Fig. 1). We chose an EF strength of 100 MV/m based on our prior experience [21,23,36] with molecular dynamics simulations of proteins with EF – although this value might seem huge microscopically, it is actually comparable to the effective EF in cell membranes due to transmembrane voltage [45] and quite small compared to the values of molecular EF (GV/m) [15,46].

The representative snapshots of the structure of kinesin with the underlying tubulin heterodimer (in short: tubulin) for a selected trajectory in each EF direction are shown in Fig. 2a-d. Our major finding is that the EF detaches kinesin from tubulin and also pulls the C-termini of the underlying tubulin. Qualitative observations are the following: the kinesin is always being detached in the direction towards the anode (+ sign of the EF). This electrophoretic effect is understandable due to the Coulomb force of EF on negative (− 5 e) kinesin net charge (see S1 in [36]). Apart from this strong and obvious EF-direction-dependent effect, we also observed that the kinesin detachment proceeded along qualitatively different pathways for each EF direction. For the X direction, the detachment of kinesin was accompanied by a strong effect on the β-tubulin C-terminus tail (CTT, unstructured part of the C-terminus starting at the residue 427): it was not only pulled away from the tubulin body, but also caused the last α-helix of the β-tubulin C-terminus to be levered away from the tubulin body so that it loses its secondary structure, see Fig. SI 1–1. In contrast, for the -X EF direction, the last α-helix was not levered from the tubulin body during the kinesin detachment, yet the CTT underwent a strong pull so the last α-helix ends up denatured. The detachment process proceeded somewhat differently for the Z and -Z EF directions and is much more stochastic than for the X and -X directions. Hence, the following descriptions of the kinesin–tubulin system represent a typical qualitative behavior, with varying details in individual trajectories. For Z, only a smaller number of trajectories resulted in kinesin detachment within our simulation time; if it occurred, the effect on CTT was milder than in the X and -X directions. Interestingly, for the -Z EF direction, the detachment of kinesin was more frequent and accompanied by pulling of both α- and β-tubulin CTT from the body of tubulin.

In addition to the qualitative differences in the detachment process observed for different EF directions, there is also a quantitative difference in terms of kinetics. To explore the speed of the kinesin detachment process, we analyzed the time evolution of two parameters: the number of residue contacts and the distance between kinesin and tubulin (see Methods for the definitions), see Fig. 2e,f. The distribution of detachment times for each EF direction is plotted in Fig. 3. It is clear that, by median, the fastest detachment occurs under an EF in the X direction, followed by -X, Z, and then -Z, as also evidenced by both the number of contacts and distance analysis. The variability of the trajectories, particularly for X, Z, and -Z EF directions, is highlighted in Fig. 2. Why are the faster kinetics observed in EFs in the X and -X EF directions than in the Z and -Z directions? At first, this might be counterintuitive because a net linear motion of a whole kinesin nanomotor proceeds towards the β-tubulin end of the microtubule, also called the microtubule plus end (here -Z direction) [37]. However, the first part of a natural detachment of kinesin proceeds along the X axis because kinesin steps proceed in a rotational manner around its stalk axis [47,48], which might explain the effective detachment along the -X EF direction. The fast detachment along the X EF direction is also related to the fact that the EF also detaches (levers open) the β-tubulin C-terminus end (including the last α-helix) of β-tubulin from the tubulin body (see 1–4 ns in the animation S06), which represents a substantial fraction of the kinesin binding site on the tubulin.

Visually observing the evolution of the K-T structure, we also found that the detachment of kinesin was accompanied by the alignment of the kinesin dipole moment with the EF vector (see endpoints in all four EF directions in Fig. 2a-d) and supplementary information - animations S06-S12. To further understand this aspect of detachment, we performed analysis focusing on the evolution of the kinesin dipole moment (DM) magnitude and its angle in time, see Fig. 4a,c. We also analyzed the dipole moment of the β-tubulin C-terminus (Fig. 4a,c), since the C-terminus also seems to be affected.

The kinesin DM magnitude fluctuated at approximately 1200 debye (D) under no-EF condition, whereas it significantly increased up to 1700 D in an EF. The strongest and fastest effect was manifested by the EF in the X direction, followed by -X, Z and -Z. The DM magnitude of β-tubulin C-terminus had the no-EF value around 500 D and increased up to 800 D at the time of detachment. Similar behavior was observed for the DM angle of kinesin and β-tubulin C-terminus, where X and -X dominate over Z and -Z EF directions. Furthermore, there seems to be a correlation between the time evolution of the number of K-T contacts and K-T distance and the DM magnitude and angle. To analyze this further, we plotted these parameters in a single figure for each trajectory, see sections SI 1–10, SI 4–1. The results showed that the DM magnitude, DM angle and number of contacts seem to be mutually correlated most strongly for 100 MV/m EF strength for all analyzed EF directions. To determine if the detachment of kinesin occurs in a characteristic range of values of DM magnitude and the angle at which kinesin detachment occurs, we plotted the distributions of the values of these parameters at the detachment time (defined as the time when the number of contacts approaches zero for the first time) - see the distributions on the right of Fig. 4a. We found that the DM magnitude increased by approximately 100–400 D at the detachment time compared with the case in which there was no EF and the mean value depends on the field direction. The DM magnitude of β-tubulin C-terminus also increased by 100–300 D by the time of the detachment. The angle of DM also changed significantly at the detachment time: the DM tilted by 40° to 80° from the no-field value for kinesin and for β-tubulin C-terminus by 40–90° X, -X, see Fig. 4c.

3.2. Both EF pull on β-tubulin C-terminus and EF torque on kinesin are crucial for detachment

The detachment of kinesin is accompanied by the effects on β-tubulin C-terminus but is there a causality relationship? In other words, is the mechanical action of EF on β-tubulin C-terminus a prerequisite necessary for the kinesin detachment from the tubulin?

To answer this question, we used the unique capability of computational simulations to fully control the system at the atomic level and restrained the tubulin heterodimer underlying the kinesin,

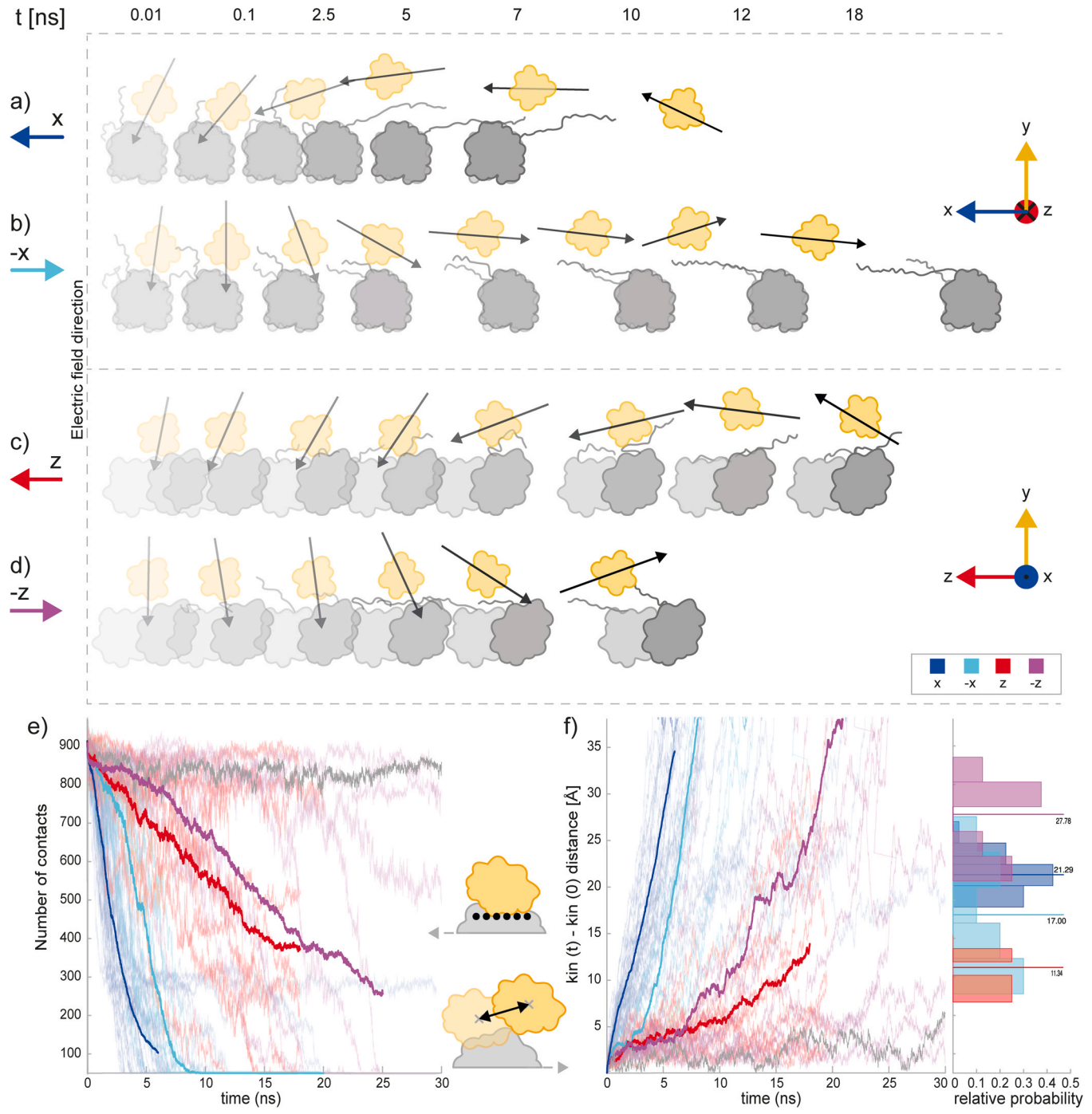

Fig. 2. Various EF directions cause different pathways of kinesin detachment. (a), (b), (c), (d) are schematic diagrams depicting a representative pathway of kinesin (in yellow) detachment from microtubule (only one heterodimer depicted for clarity - α tubulin light gray, β tubulin dark gray) for a 100 MV/m EF in the X, -X, Z, and -Z directions, respectively. See supplementary information (animations S06-S12) for molecular details or load the raw trajectories we share to any molecular viewer for the full 3D information. e) The number of contacts between kinesin and tubulin. (f) The distance kinesin is displaced relative to the position at time zero of the simulation is a metric of kinesin–tubulin distance. Distributions on the right are from individual simulations and show the values of the kinesin distance at the time of the detachment (i.e., when zero number of contacts between kinesin and tubulin was reached), straight lines show the mean of the distribution.

which would be practically impossible in experiments. Under such conditions, all tubulin α-carbon atoms were held in place so that the EF could practically affect only the kinesin atoms. The simulations were carried out under these conditions for the 100 MV/m EF, -X direction. We found (Fig. SI 1–2) that the detachment effect was dramatically reduced and delayed: only three out of ten trajectories showed a sign of kinesin detachment within 10 ns. These findings demonstrate that the displacement action of EF on the β-tubulin C-terminus is crucial for the effect observed under our EF conditions.

As we observed the rotation of kinesin and alignment of its dipole moment with EF, we wanted to dissect the pure pulling (EF-induced linear force due to the net charge of kinesin) and rotation (EF-induced torque due to the kinesin dipole) effects. To distinguish the mere pulling and rotation effect of the EF on the kinesin, we compared the effect of the pure pulling force with the electric force. We pulled the center of mass of the kinesin by a constant force (80.1 pN, the same force due as $F = |q_t . E|$, where q_t is the net kinesin charge, see section SI 1–3) in the -X direction. We found (see Fig. SI

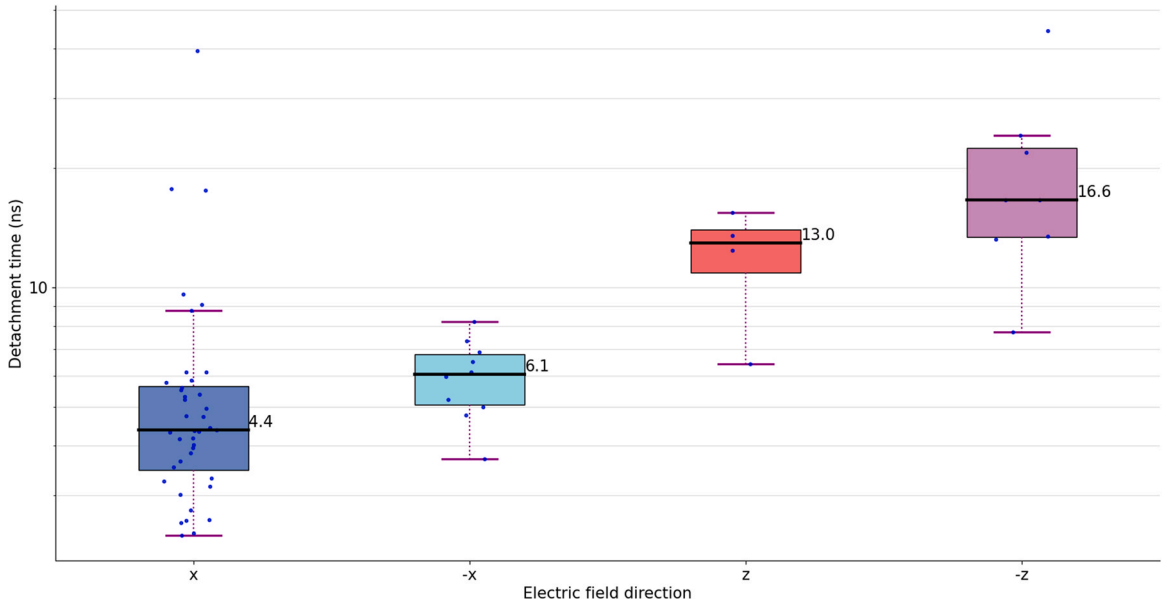

Fig. 3. Box plots of detachment times of the kinesin motor domain from tubulin for 100 MV/m X, -X, Z, and -Z EF direction. Dots represent individual data points. Black lines are medians. The statistical significance of differences between X and -X EF directions data has $p < 0.05$ (Kolmogorov-Smirnov test), other data could not be tested due to a low number of data points, see Section SI 1–9.

1–3) that while the pulling force itself does not detach kinesin, the EF does. These findings indicate that other EF force components, probably the torque, are crucial for the detachment to occur.

To understand this quantitatively, we analyzed the work carried out by the EF on kinesin and β-tubulin C-terminus decomposed to a translation and rotation component, Fig. 4b,d. For each EF direction, the kinetics of the translation work exerted on the β-tubulin C-terminus dominates the work exerted on kinesin. The kinetics of the rotational work is dominated by the contribution of kinesin over the β-tubulin C-terminus from the beginning of the simulation for X and -X EF directions, but for Z and -Z EF directions, the dominance became visible only in later stages after 5 ns. The mean of the distributions in Fig. 4b,d enables ranking of the contributions of translational work, rotational work on kinesin and β-tubulin C-terminus at the moment of kinesin detachment. β-tubulin C-terminus. As the distribution is very wide and hence barely visible for X β-tubulin C-terminus (dotted blue line distribution) in Fig. 4b,d, see Fig. SI 1–6 for the individual depiction of distributions.

In general, it is the translation work on the β-tubulin C-terminus tail and the rotational work on the kinesin dipole that is dominant for the detachment, see Fig. SI 1–5. This is corroborated by our above findings that, during the detachment:

1. the kinesin
   (a) dipole moment magnitude (hence the force of EF and work) is higher than that of the tubulin tail (Fig. 4
   (b) dipole rotation hence also the rotation of whole protein is observed (Fig. 2) and required (Fig. SI 1–2) for the detachment
2. the β-tubulin C-terminus
   (a) net charge is almost 4-fold higher than that of the kinesin (− 19 e vs. − 5 e, see Section SI 1–3)
   (b) mobility constraint hampers the kinesin detachment (Fig. SI 1–2)

3.3. Electric field causes kinesin detachment in a field strength-dependent manner

In all further work presented here, we focused on the X EF direction as it seems to be effective for kinesin detachment (Fig. 3, 4). To understand the energetics of the kinesin–tubulin interaction, we calculated the potential of the mean force as a function of X-Y kinesin-tubulin distance along the detachment trajectory, see Fig. SI 1–13. We see that starting from a K-T distance of 7 nm (calculated as the distance between the geometrical centers of the kinesin and tubulin heterodimer), that is, 2 nm from the initial distance (5 nm), there is almost zero interaction energy. This finding reasonably justifies the zero number of contacts criterion as the criterion for the detachment – as shown in Fig. 2, the K–T distance at the time of kinesin detachment is indeed approximately 2 nm (20 Å) for the X EF direction.

The pertinent question was: how does the EF strength affect the kinesin detachment process? To answer this, we ran the simulations for the EF in the X direction for field strengths of 30, 50, 75 MV/m, in addition to the data for 100 MV/m shown above (see all results in Fig. 5). The time evolution of the number of contacts and K–T distance demonstrate that the kinetics of detachment slows and becomes more stochastic with decreasing EF strength, Fig. 5a,b. Similarly, the DM magnitude and angle of both kinesin and β-tubulin C-terminus also manifested EF-dependent time evolution. The kinesin DM magnitude at the detachment time depends on the EF strength: an EF strength of 100 MV/m increases the DM magnitude by approximately 30 % compared with no-field conditions, whereas an EF strength of 30 MV/m EF had a negligible effect on the DM magnitude (Fig. 5c). Although EF also affected the DM magnitude of the β-tubulin C-terminus in an EF-strength dependent manner, there is only a small variation of the mean DM magnitude values at the time of the detachment (from 680 D at 100 MV/m to 754 D at 30 MV/m, see distributions on the right of Fig. 5c) across different EF strength values. However, there is quite some variation within the data at a particular field strength.

The change of the kinesin DM angle is also EF-dependent. However, the values of the DM angle at the detachment time were slightly less spread than the DM magnitude values, and even 30 MV/m can exert substantial influence on the angle, albeit often this has to be accumulated over a longer time scale (Fig. 5d). These results suggest that the change of the DM magnitude is not necessary for the detachment, whereas tilting the kinesin (the change of angle) seems to be much more important. This is supported by the analysis of time evolution of individual parameters for 30 MV/m EF, see

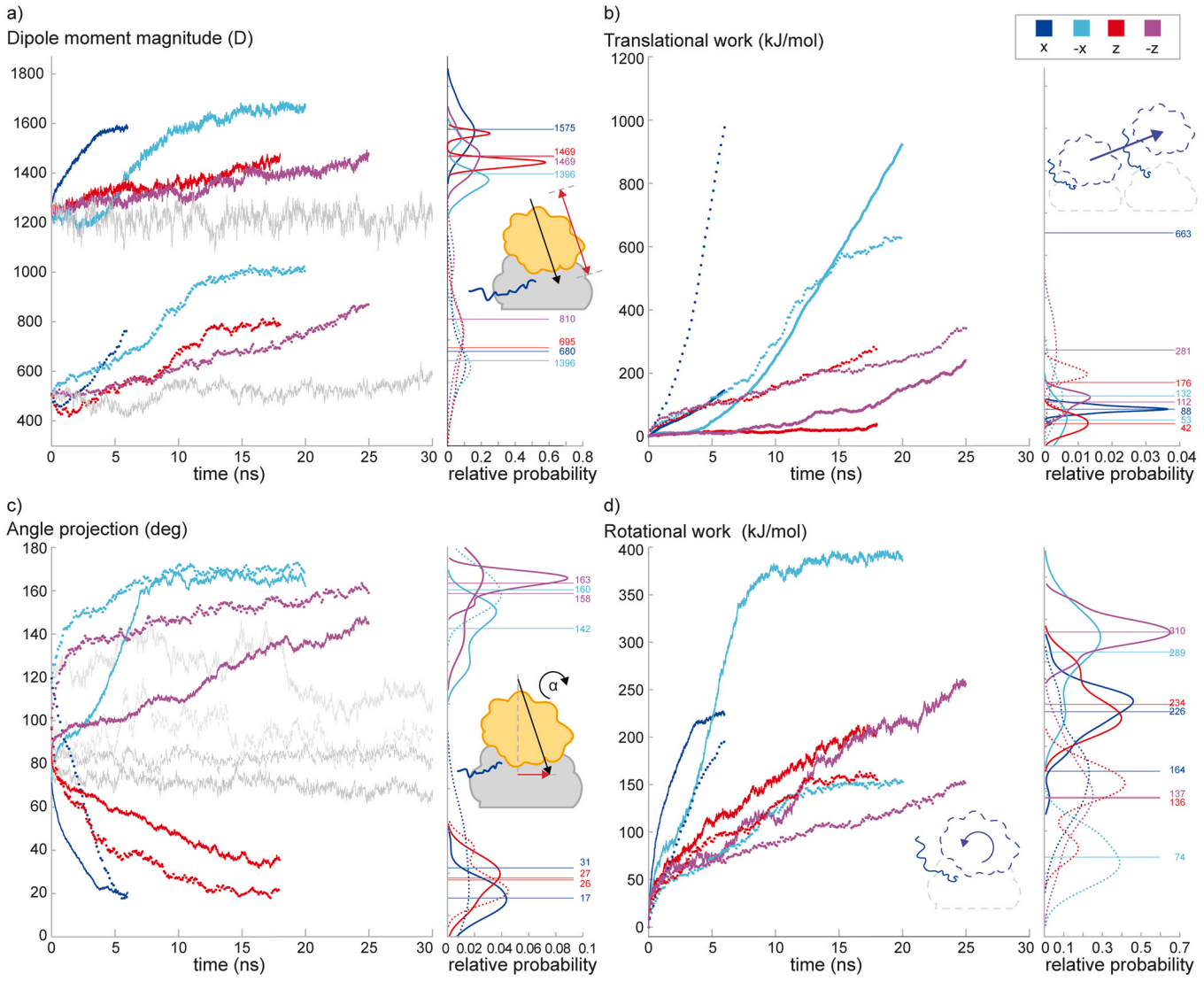

Fig. 4. Effects of 100 MV/m EF on kinesin (solid line) and β-tubulin C-terminus (dotted line) for various EF directions. a) Kinetics of the dipole moment magnitude and c) angle projection (see Eqs. (2) and (3)). b) translational and d) rotational work carried out by the EF on the protein. Color coding: X (blue), -X (cyan), Z (red), and -Z (violet) EF directions and gray is the trajectory with no EF. The colored lines are the mean from N = 40 for X, N = 10 for -X, N = 10 for Z, N = 10 for -Z trajectories. In c), the gray lines are the reference (no EF) trajectories: solid dark gray and solid light gray for kinesin and β-tubulin C-terminus respectively, in X and -X EF direction (from Eq. (2)), dashed dark gray and dashed light gray for kinesin and β-tubulin C-terminus respectively, in Z and -Z EF direction (from Eq. (3)). Distributions on the right display relative probability of the occurrence and the mean of the value for each quantity at the time when zero number of contacts between kinesin and tubulin (see Fig. 2e) was reached. For example, in a), for the trajectories with X EF direction, the value of the kinesin dipole moment magnitude at the time when zero number of contacts was reached was between 1400 D and 1750 D and the mean value was 1575 D. The probability density functions were obtained by fitting with kernel density estimation utilizing MATLAB 2021a histfit function with five bins.

section SI 3–2, where often the change of number of contacts and DM angle is substantial, whereas almost no change of DM magnitude occurs, see e.g., Fig. SI 3–29 or SI 3–30. Nevertheless, the torque depends on the DM magnitude, so necessarily the increase of the DM magnitude increases the torque and has to facilitate the detachment. Overall, these results underline the importance of the EF torque action for the kinesin detachment process. The behavior of the β-tubulin C-terminus DM angle is different from the kinesin DM angle. The change of the DM angle during the action of EF from the start of the simulation until the time of the detachment is much higher for the β-tubulin C-terminus (from 120° to 20°) at 100 MV/m than for kinesin (from 70° to 20°), which is due to the high flexibility of this part of tubulin. Also, the spread of the DM angle values at the time of the detachment for each field strength is much wider than that for kinesin.

Subsequently, we analyzed the rotational and translational components of work carried out by EF on the kinesin and β-tubulin C-terminus (Fig. 5e,f) for various EF strength values for an EF in the X direction. The rotational work on kinesin and the translational work on the β-tubulin C-terminus evolved comparably until 1 ns, but then the translational work of EF on the β-tubulin C-terminus takes over and is the major contribution to the total work carried out at the time of the detachment Fig. SI 1–5. Nevertheless, the work carried out by EF on kinesin is also substantial (Fig. SI 1–5). We found that the rotational component had a higher value than the translational one. However, the ratio of rotational to translational decreased with decreasing EF strength – what are the reasons for this trend? There are at least two reasons: the first one is the fact that the DM change is lower, and hence the rotational work is also lower at lower EF strength. The second reason is that the change of the dipole angle, which is proportional to the rotational work, is also lower at lower EF strength compared to higher EF strength.

Finally, we analyzed the dependence of the time required to detach the kinesin on the applied EF strength, see Fig. 6a. The detachment time decreased with increasing field strength, as expected because a higher field strength will act by a larger force, hence

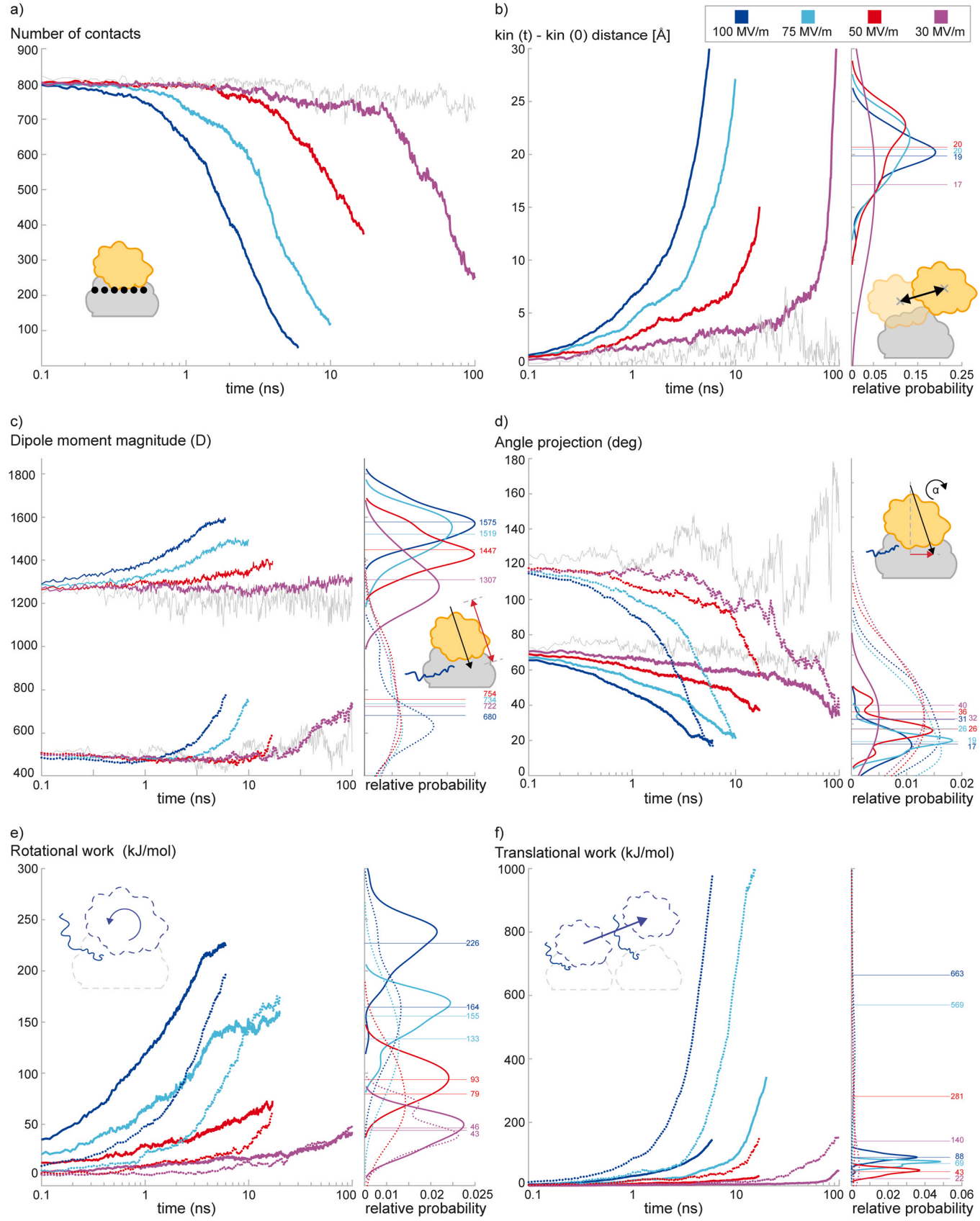

Fig. 5. Dependence of the electric field effects on the kinesin (solid lines) and β-tubulin C-terminus (dotted lines) on the EF strength for the X EF direction. Kinetics of a) the number of contacts between kinesin and tubulin, b) the kinesin displacement. c) the kinesin and β-tubulin C-terminus dipole moment magnitude d) the dipole angle projection, e) rotational, and f) translational work carried out by the EF on the kinesin and β-tubulin C-terminus. Color coding: 100 MV/m (blue), 75 MV/m (cyan), 50 MV/m (red), and 30 MV/m (violet) electric field strength and gray is the trajectory with no EF. The colored lines are the mean from N = 40 for 100 MV/m, N = 30 for 75 MV/m, N = 20 for 50 MV/m, N = 10 for 30 MV/m trajectories. The density functions were obtained from kernel density estimation utilizing MATLAB 2021a histfit function with five bins.

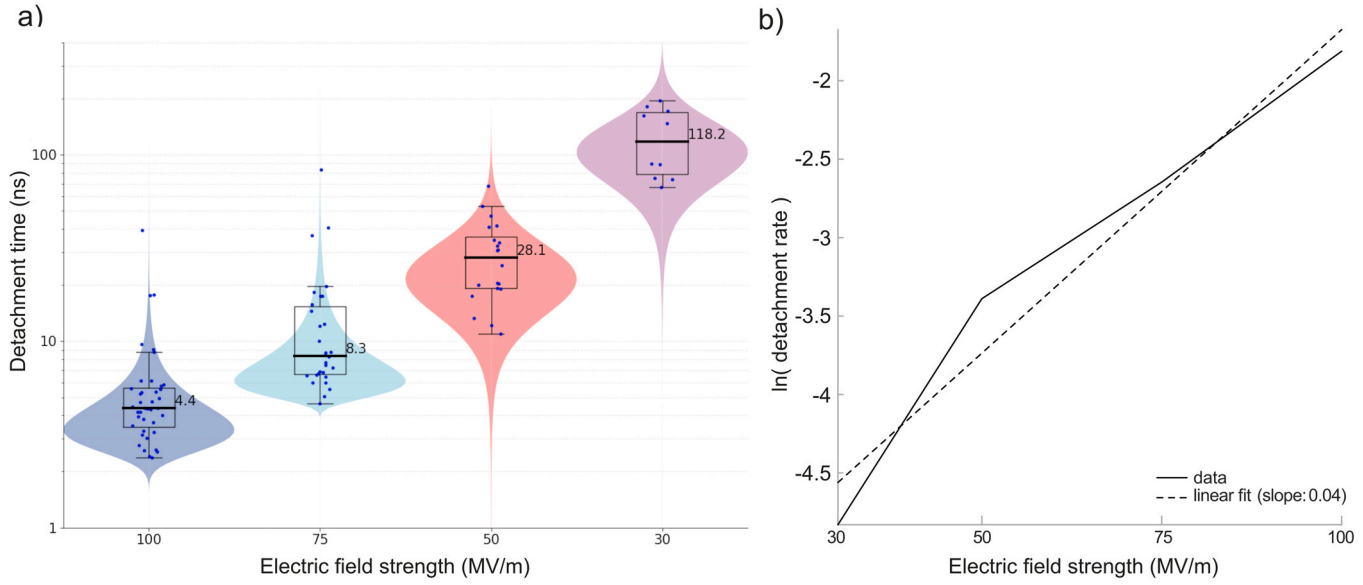

Fig. 6. a) Distributions (alpha distributions fit – Eq. SI 1–1) and box plots of detachment times of kinesin motor domain from tubulin for 30, 50, 75, and 100 MV/m EF strength (all in X direction). Dots represent individual data points, the black line in box plot is median. The statistical significance of differences between individual pairs of data sets has $p < 0.05$ (Kolmogorov-Smirnov test), see Section SI 1–9 for details. b) Natural logarithm of detachment rate (1/detachment time, considering time in ns) plotted against EF strength with a linear fit. The intercept from the fit is at − 5.8.

increasing the probability of kinesin detachment. This direction of the effect can be intuitively understood, but how do we quantitatively relate these results in terms of energetics?

3.4. Electric field affects the kinesin detachment rate

To conceptually understand the EF-strength dependence in terms of the energetics underlying the rate of kinesin detachment (dissociation) from MT, we can apply the Arrhenius equation [49,50] (assuming a single activation energy barrier)

$$k_{OFF_0} = A e^{-\frac{\Delta E_a}{k_B T}} \tag{8}$$

where k_{OFF_0} is the rate of detachment at zero EF, A is a preexponential factor, k_B is the Boltzmann constant, T is the absolute temperature and ΔE_a is the height of the activation energy barrier. The external force applied along the reaction coordinate modifies the Arrhenius equation [51]. Within this framework, we propose that when the EF force is considered, the activation barrier can be altered (lowered in our case) and we may write

$$k_{OFF}(E) = A e^{-\frac{(\Delta E_a - E I_E)}{k_B T}} = k_{OFF_0} e^{\frac{I_E}{k_B T} E} \tag{9}$$

where E is the external EF and I_E is the term that describes the EF interaction with the system, having units of [C.m]. We consider that the detachment time t_{OFF} in Fig. 6 is related to the detachment rate as $k_{OFF} = 1/t_{OFF}$ and we plotted the natural logarithm ln() of the rate having on the vertical axis, since the ln() transforms the exponential form of the equation to a linear one, enabling easier processing,

$$\ln k_{OFF}(E) = \ln k_{OFF_0} + \frac{I_E}{k_B T} E \tag{10}$$

see Fig. 6. Then, we determined the value of the slope I_E/k_BT by fitting to be 0.04 (using ns and MV/m), which, using the units of s and V/m, translated to the value of the slope 4×10^{-8} [m/V], hence $I_E = 1.85 \times 10^{-28}$ [C.m]. The value of the interaction term quantitatively informs about the degree to which EF couples with the system to lower the activation energy barrier E_a. Where does this interaction term arise from? We know from the results earlier in this paper that EF exerts both rotational work (through torque) on kinesin and β-tubulin C-terminus dipole) and also translational work (through kinesin and β-tubulin C-terminus charge) play a role in the kinesin detachment. Therefore, we reasonably expect that the interaction term will be proportional to the following components:

$$I_E \simeq (p_P + p_I)\,\Delta\cos\Phi + q\,\Delta x \tag{11}$$

where p_P is the magnitude of permanent DM of the protein, p_I is the DM induced due to structural changes of the protein, $\Delta\cos\Phi = \cos\Phi_{END} - \cos\Phi_{START}$, where Φ_{END} is the ending angle and Φ_{START} is the starting angle between the EF and the DM vector, q is the charge of the protein and Δx is the distance change during the transition.

We made independent analytical estimates of the order of magnitude of the values of interaction terms, see Table 2. These estimates were approximately two orders of magnitude higher than the value found from the molecular dynamics simulations (Fig. 6b). That means that some of the quantities involved were effectively lower in MD simulations than in the analytical estimates.

The exact underlying reason is likely complex. However, we argue here that the most impotant factor is the dielectric screening. If we consider the protein in water from the perspective of electrostatics, a protein represents a cavity in dielectric material (water, here the TIP3P has a static dielectric constant ε of ca. 101 [52]. We assume that the effective dielectric constant of protein is close to 1 since we use non-polarizable force field in our MD simulations. In such case the field in the center of the cavity is given by $E_{CAV} = 3 / (2\varepsilon + 1)\, E_{EXT}$ [53].

Table 2
Analytical estimates of the values of the terms (values are in 10^{-28} [C.m]) that facilitate the kinesin detachment due to the kinesin and β-tubulin C-terminus dipole and charge coupling with an EF. Assumed values for the kinesin: $p_P = 1200$ D, $p_I = 130$ D, $q = -5$ e, $\Delta x = 2$ nm, for the β-tubulin C-terminus: $p_P = 500$ D, $p_I = 150$ D, $q = -19$ e, $\Delta x = 2$ nm. For the kinesin (and β-tubulin C-terminus), the DM angle β with respect to the EF vector changes from ca. 80° to 20° (and from 120° to 30°) by the time of detachment, see. See the details of the calculations in Supplementary information 5.

term	kinesin	β-tubulin C-terminus
p_P	31	23
p_I	3	7
$q\,\Delta x$	16	61
sum	50	91

E_{CAV} corrresponds to the effective EF strength acting on a protein and $_{EEXT}$ is the value of the EF strength we apply in MD simulation. The ratio of $E_{CAV}/_{EEXT}$ from the equation above is 0.0148 which is an excellent agreement with the ratio of the $I_{E\text{-}MD}$ / $I_{E\text{-}Analytical}$ = 1.85/141 = 0.013. 141 is the sum of contribution from the kinesin (50) and tubulin (91) from the Table 2. This result underlines the effect of dielectric screening in the EF effects on proteins.

3.5. Discussion: prediction of the effect on kinesin function

Our MD simulation results indicate that EF facilitates ADP-bound kinesin motor domain (head) detachment (dissociation) from MTs. The effect is due to both the direct effect on the kinesin as well as on the β-tubulin C-terminus. Lets first discuss the major outcome – the detachment of the kinesin motor domain (head). How would this detachment affect the function of the whole kinesin and how can these results be verified experimentally? The minimal functional state of the kinesin-1 comprises a dimer (Fig. 1) that undergoes a complex mechano-chemical cycle [5] that generates a directional movement on MTs, so we can not interpret the results in isolation. There are several potential fates of a single kinesin dimer after the kinesin head is detached. One option is that the second head is also detached by the EF, if not already untethered during the kinesin stepping, and the whole kinesin dimer dissociates from the MT. The second option is that in a certain parameter range of EF strength and EF application duration, it could happen that the EF would detach one head and the second would remain tethered to the MT. If the EF acted further and pulled the detached kinesin away, it might initiate the dissociation of the two monomers of kinesin from each other by unzipping the connecting neck linker. The third option offers a whole range of possibilities based on the assumption that the second motor domain remains tethered to the MT and kinesin retains its dimeric state. The outcome depends on when (in the phase of the kinesin stepping cycle) the EF hits the system, and EF direction and strength: .

1. speed up the detached head diffusion to facilitate the step (-Z EF direction facilitating the forward (along Z axis direction) motion of the negatively charged kinesin head)
2. hold back the free head (would require much longer EF duration than the 1HB state (~ 3 ms) [5], when the free head is diffusively searching for the landing site of the next step) and slow down the whole step (-Z EF direction)
3. the kinesin would side-step on the neighboring protofilament (X and -X EF)
4. when the EF is switched off, the detached head would re-attach back to the same spot on MT

Combining some of these effects, one can imagine a time and space-tailored EF to facilitate fast detachment (X EF direction) and then speed up the diffusive search of kinesin to the next docking position (Z EF direction). Furthermore, the EF can act on many kinesin motors in parallel, hence it could be used to create effects such as synchronization of kinesin stepping. Although most of the kinesin motors are dimeric, there are also kinesin motors that operate as monomers such as KIF1A [54]. Such motors do not operate in a hand-over-hand motion, as the dimeric kinesins, but diffusively progress along the MTs interacting with the charged C-terminus of tubulin [55] and work cooperatively in teams to transport the cargo [56]. If the monomeric kinesin is exposed to a sufficiently intense EF, the effects could be more straightforward than for the dimeric kinesin: the detachment of the single head would lead to the dissociation of the motor from its microtubule track, since there would be no second head to keep the motor anchored on the microtubule.

Mastering these EF effects on kinesin would have a significant impact on bionanotechnology, where the control of nanomotors is desired. On the other hand, an EF could be used as an additional load to explore the function of the kinesin itself. For example, an EF applied in the Z or -Z direction would act as an assisting or hindering load facilitating or hindering the step of the kinesin, which could be used to explore the role of neck linker, such as in [57].

Future analysis should include kinesin states where ATP is bound to the kinesin motor domain (ATP-state) or no nucleotide at all (APO-state). It is known there is a higher contact surface area and also stronger binding of kinesin motor domain to an MT in ATP-state and also APO-state than in ADP-state [42]. Therefore, we expect that a higher EF strength or EF application time would be required to detach the kinesin motor domain for ATP-state and APO-state, than for ADP-state.

3.6. Discussion: EF effects on kinesin in vitro vs. in vivo

While the potential effects of EF on kinesin in vitro are elaborated above, here we discuss potential implications in vivo. The only work that has addressed the question of effects of the intense pulsed EF in vivo focused on plant-specific KCH kinesin from the kinesin-14 family [58]. There, N = 25 of 25 ns pulses of EF strength up to 1 MV/m were applied to BY2 cells and the effect of EF together with overexpression of KCH kinesin was evaluated. The authors concluded, that the nanosecond pulsed EF targets, apart from the membrane, also the microtubule-KCH-actin cross-linking complex. However, the complexity of the biological response to pulsed EF obscures this interpretation. These in vivo results beg for in vitro experiments, where individual components (MTs, actin and kinesin cross-linking domain) can be reconstituted under well-controlled out-of-the cell environment. In such reconstituted systems, any observed effect of pulsed EF would provide a more convincing and cleaner interpretation and would complement the observations from in in vivo experiments.

3.7. Discussion: EF effects on tubulin

Next, we discuss the effects of EF on the tubulin heterodimer that binds the kinesin. The major effects we saw were on the C-terminus tail of the tubulin, particularly that of β-tubulin, which carries a higher electric charge than that of α-tubulin. Earlier works on a tubulin heterodimer in an EF [21,23,33] corroborate these findings. The free tubulin shows the displacement of loose, charged segments, including the C-termini tails, in response to EF up to 75 MV/m [33]. In [21], an EF starting from 20 MV/rotates the free tubulin, significantly pulls the C-terminus starting from 50 MV/m and denaturation of the secondary structures (α-helices on the C-terminus end of tubulin) was observed only for very high EF strengths (300 MV/m). In our recent work [23], where the whole microtubule lattice was analyzed in an EF, no denaturation effects were observed on the level of individual tubulin in the MT lattice were observed. In light of these earlier data, it is very interesting that in this work, we observed the denaturation of one tubulin, particularly the α-helix proximal to the C-terminus of the β-tubulin, already at an EF strength of 100 MV/m in the X-direction, see SI 1–1. We suggest that the binding of the kinesin to the last α-helix of the β-tubulin [59] and the rotational force (torque) on the kinesin facilitates the levering of the α-helix from the tubulin body and its denaturation, additional to the EF pull on tubulin C-terminus charge. From the tubulin-centric perspective, this suggestion means that the presence of the kinesin bound to the tubulin renders the tubulin more susceptible to an EF, since the kinesin represents another handle through which the tubulin can be affected. Interestingly, the denaturation of the last tubulin occurred at an EF field strength of 100 MV/m in the X and -X direction but was practically absent in the Z and -Z EF directions.

3.8. Discussion: ionic strength, heating and electrochemistry

Our simulations included physiologically relevant concentrations of ions (K^+ and Cl^-) and water, see Table 1. Therefore, the effect of an EF on ions and water is included in the effects we observed. We did not carry out any particular analysis on the dynamics of ions and water, but visualizing the trajectory we observe that (i) ions undergo electrophoretic motion and (ii) water undergoes polarization to align with an external EF. In our earlier work [23], we found no significant effect of ionic strength on the electro-opening of MT, i.e., the detachment of two neighboring tubulin molecules by EF. Instead, the EF effects were mainly due to the effect on protein charges and dipole moments. Therefore, we speculate that ionic strength is not a crucial parameter in our current simulation work, except for the heating of the system. The system in our simulations is coupled to external thermostat keeping the temperature constant. This situation corresponds to real experiment in laboratory conditions where the system is in thermal contact with its surrounding. In an experiment, the actual temperature change would depend on the input heating power delivered by the EF (which is related to the effective conductivity of the sample) and heat dissipation from the sample. Practically, heating effects are mostly negligible when EF of MV/m scale is applied on the nanosecond timescale [28]. The electrochemical effects depend on the amount of charge that flows through Faradaic currents. When an EF is delivered in pulses on the nanosecond timescale, a large proportion of the total current is of capacitive character and does not involve Faradaic charge transfer that causes electrochemical effects. Apart from the pulse duration, it is the conductivity and dielectric properties of the sample as well as material of the electrode that modulates the proportion of Faradaic versus capacitive currents. Therefore, to get close to the simulation conditions in experiments, one has to appropriately set the parameters of the experiment (EF parameters, geometric, material, and sample arrangements), but they seem to be physically and technical achievable.

3.9. Discussion: proposed experimental tools for verification

Overall, our computational results have a profound importance for the guidance of the experimental design: not only EF strength, but also EF direction, with respect to the microtubule and kinesin orientation, significantly affect the detachment process. To experimentally verify the predictions, one would ideally need to collect the data from single-molecule imaging techniques, such as TIRF microscopy [60], but with a high temporal resolution to resolve EF effects within the time step, such as iSCAT [61–64]. Furthermore, suitable chip technology is required that integrates microfluidics for the sample position and manipulation, electrodes system capable of delivering high EF strengths at sufficiently broad frequency bandwidth (required for ns and shorter electric pulses) and compatibility with the advanced microscopy techniques mentioned above. The integrated technology platforms presented, e.g., in [30,65], fulfill all such requirements when coupled to proper imaging techniques.

Finally, the electric-field-modified activation energy model is an important first step towards understanding the relationship between the EF strength and the time scales needed to observe the effects of the electromagnetic field at the molecular scale. The model conceptually enables scaling of the effects of the EF down to a lower field strength experienced by kinesin in an organism under a variety of circumstances, such as exposure to an electromagnetic field generated by various telecommunication or industrial devices. Therefore, it would be of interest for bioelectromagnetics research.

4. Conclusion

Molecular dynamics simulations were used to show that an intense EF can be used to detach the motor domain of a kinesin nanomotor from its microtubule track. We demonstrated that this effect depends on the EF direction as well as EF strength. Different EF orientations tend to detach kinesin via different pathways, but overall the X EF direction (i.e., perpendicular to the direction of kinesin transport, and parallel to the microtubule surface) was shown to be the most effective for kinesin detachment. During the detachment process, the number of contact residues between kinesin and tubulin decreases, while the mutual distance between them increases. We suggest that the major mechanism of detachment is the action of EF on the β-tubulin C-terminus charge and kinesin dipole moment, as demonstrated by the effect on its magnitude and angle. This was confirmed by the finding that the rotational component of the work carried out by EF on kinesin-1 was found to be dominant over the translational component. We introduced an Arrhenius-equation-based model to interpret the rate of detachment at various EF strengths. The results provide a better understanding of the EF–kinesin interaction and highlight the directions for future work. Finally, based on our findings, we discussed potential effects of the EF on kinesin nanomotor function in terms of applications in bionanotechnology and bioelectromagnetics, once the experimental data for our computational predictions are available.

Conflicts of interest

There are no conflicts of interest to declare.

Acknowledgments

The authors thank the Czech Science Foundation project no. 20–06873X for the major support. Computational resources were supplied by the project "e-Infrastruktura CZ" (e-INFRA CZ LM2018140) supported by the Ministry of Education, Youth and Sports of the Czech Republic. Neuron collective is acknowledged for graphical design and The Science Editorium for manuscript structure and language check. The authors generated the Introduction section in a small part with text-davinci-003, OpenAI's large-scale language-generation model. Upon generating draft language, the authors reviewed, edited, and revised the language to their own liking and take ultimate responsibility for the content of this publication.

CRediT authorship contribution statement

Jiří Průša: Data curation, Formal analysis (lead), Investigation (lead), Methodology, Software, Visualization, Writing - original draft (supporting), Writing - review & editing (supporting). **Michal Cifra**: Conceptualization, Formal analysis (supporting), Funding acquisition, Investigation (supporting), Project administration, Resources, Supervision, Validation, Visualization (supporting), Writing - original draft (lead), Writing - review & editing (lead).

Appendix A. Supporting information

Supplementary data associated with this article can be found in the online version at doi:10.1016/j.csbj.2023.01.018.

References

[1] Miki H, Okada Y, Hirokawa N. Analysis of the kinesin superfamily: insights into structure and function. Trends Cell Biol 2005;15:467–76. https://doi.org/10.1016/j.tcb.2005.07.006⟨https://www.sciencedirect.com/science/article/pii/S0962892405001820⟩.

[2] Verhey KJ, Hammond JW. Traffic control: regulation of kinesin motors. Nat Rev Mol Cell Biol 2009;10:765–77. https://doi.org/10.1038/nrm2782⟨http://www.nature.com/articles/nrm2782⟩.

[3] Wordeman L. How kinesin motor proteins drive mitotic spindle function: Lessons from molecular assays. Semin Cell Dev Biol 2010;21:260–8. https://doi.org/10.1016/j.semcdb.2010.01.018⟨https://www.sciencedirect.com/science/article/pii/S1084952110000194⟩.

[4] Fan R, Lai K-O. Understanding how kinesin motor proteins regulate postsynaptic function in neuron. FEBS J 2022;289:2128–44. https://doi.org/10.1111/febs.16285

[5] Hancock WO. The kinesin-1 chemomechanical cycle: stepping toward a consensus. Biophys J 2016;110:1216–25. https://doi.org/10.1016/j.bpj.2016.02.025⟨http://linkinghub.elsevier.com/retrieve/pii/S0006349516002137⟩.

[6] Chandrasekaran G, Tátrai P, Gergely F. Hitting the brakes: targeting microtubule motors in cancer. Br J Cancer 2015;113:693–8. https://doi.org/10.1038/bjc.2015.264.⟨https://www.nature.com/articles/bjc2015264⟩. bandiera_abtest: a Cc_license_type: cc_y Cg_type: Nature Research Journals Number: 5 Primary_atype: Reviews Publisher: Nature Publishing Group Subject_term: Chemotherapy;Kinesin;Microtubules;Mitosis Subject_term_id: chemotherapy;kinesin;microtubules;mitosis.

[7] Musumeci O, Bassi MT, Mazzeo A, Grandis M, Crimella C, Martinuzzi A, et al. A novel mutation in KIF5A gene causing hereditary spastic paraplegia with axonal neuropathy. Neurol Sci 2011;32:665–8. https://doi.org/10.1007/s10072-010-0445-8

[8] Goizet C, Boukhris A, Mundwiller E, Tallaksen C, Forlani S, Toutain A, et al. Complicated forms of autosomal dominant hereditary spastic paraplegia are frequent in SPG10. Hum Mutat 2009;30:E376–85. https://doi.org/10.1002/humu.20920

[9] Hess H, Howard J, Vogel V. A Piconewton forcemeter assembled from microtubules and kinesins. Nano Lett 2002;2:1113–5. https://doi.org/10.1021/nl025724i

[10] Nitzsche B, Ruhnow F, Diez S. Quantum-dot-assisted characterization of microtubule rotations during cargo transport. Nat Nanotechnol 2008;3:552–6. https://doi.org/10.1038/nnano.2008.216

[11] Isozaki N, Shintaku H, Kotera H, Hawkins TL, Ross JL, Yokokawa R. Control of molecular shuttles by designing electrical and mechanical properties of microtubules. Sci Robot 2017;2:eaan4882. https://doi.org/10.1126/scirobotics.aan4882

[12] Nicolau DV, Lard M, Korten T, van Delft FCMJM, Persson M, Bengtsson E, et al. Parallel computation with molecular-motor-propelled agents in nanofabricated networks. Proc Natl Acad Sci USA 2016;113:2591–6. https://doi.org/10.1073/pnas.1510825113

[13] Grant BJ, Gheorghe DM, Zheng W, Alonso M, Huber G, Dlugosz M, et al. Electrostatically biased binding of kinesin to microtubules. PLOS Biol 2011;9:e1001207. https://doi.org/10.1371/journal.pbio.1001207

[14] Tsai M-Y, Zheng W, Balamurugan D, Schafer NP, Kim BL, Cheung MS, et al. Electrostatics, structure prediction, and the energy landscapes for protein folding and binding: electrostatic Energy Landscapes for Folding and Binding. Protein Sci 2016;25:255–69. https://doi.org/10.1002/pro.2751

[15] Fried SD, Bagchi S, Boxer SG. Extreme electric fields power catalysis in the active site of ketosteroid isomerase. Science 2014;346:1510–4.

[16] Li L, Jia Z, Peng Y, Godar S, Getov I, Teng S, et al. Forces and disease: electrostatic force differences caused by mutations in kinesin motor domains can distinguish between disease-causing and non-disease-causing mutations. Sci Rep 2017;7:8237. https://doi.org/10.1038/s41598-017-08419-7⟨http://www.nature.com/articles/s41598-017-08419-7⟩.

[17] Zhang Z, Witham S, Alexov E. On the role of electrostatics in protein–protein interactions. Phys Biol 2011;8:035001. https://doi.org/10.1088/1478-3975/8/3/035001⟨http://stacks.iop.org/1478-3975/8/i=3/a=035001?key=crossref.77ff819e2185726797249d4b9bc237c4⟩.

[18] Ciudad A, Sancho JM, Tsironis GP. Kinesin as an electrostatic machine. J Biol Phys 2007;32:455–63. https://doi.org/10.1007/s10867-006-9028-6

[19] Hekstra DR, White KI, Socolich MA, Henning RW, Šrajer V, Ranganathan R. Electric-field-stimulated protein mechanics. Nature 2016;540:400–5. https://doi.org/10.1038/nature20571⟨https://www.nature.com/articles/nature20571⟩.

[20] Ho SY, Mittal GS, Cross JD. Effects of high field electric pulses on the activity of selected enzymes. J Food Eng 1997;31:69–84. https://doi.org/10.1016/S0260-8774(96)00052-0⟨https://www.sciencedirect.com/science/article/pii/S0260877496000520⟩.

[21] Marracino P, Havelka D, Průša J, Liberti M, Tuszynski J, Ayoub AT, et al. Tubulin response to intense nanosecond-scale electric field in molecular dynamics simulation. Sci Rep 2019;9:10477. https://doi.org/10.1038/s41598-019-46636-4

[22] Jiang Z, You L, Dou W, Sun T, Xu P. Effects of an electric field on the conformational transition of the protein: a molecular dynamics simulation study. Polymers 2019;11:282. https://doi.org/10.3390/polym11020282.⟨https://www.mdpi.com/2073-4360/11/2/282⟩. number: 2 Publisher: Multidisciplinary Digital Publishing Institute.

[23] Průša J, Ayoub AT, Chafai DE, Havelka D, Cifra M. Electro-opening of a microtubule lattice in silico. Comput Struct Biotechnol J 2021;19:1488–96. https://doi.org/10.1016/j.csbj.2021.02.007⟨https://www.sciencedirect.com/science/article/pii/S2001037021000581⟩.

[24] English NJ, Mooney DA. Denaturation of hen egg white lysozyme in electromagnetic fields: a molecular dynamics study. J Chem Phys 2007;126:091105. https://doi.org/10.1063/1.2515315

[25] English NJ, Waldron CJ. Perspectives on external electric fields in molecular simulation: progress, prospects and challenges. Phys Chem Chem Phys 2015;17:12407–40. https://doi.org/10.1039/C5CP00629E⟨http://xlink.rsc.org/?DOI=C5CP00629E⟩.

[26] Zhao W, Yang R. Experimental study on conformational changes of lysozyme in solution induced by pulsed electric field and thermal stresses. J Phys Chem B 2010;114:503–10. https://doi.org/10.1021/jp9081189

[27] Zhang S, Sun L, Ju H, Bao Z, Zeng X-a, Lin S. Research advances and application of pulsed electric field on proteins and peptides in food. Food Res Int 2021;139:109914. https://doi.org/10.1016/j.foodres.2020.109914⟨https://www.sciencedirect.com/science/article/pii/S096399692030939X⟩.

[28] Chafai DE, Sulimenko V, Havelka D, Kubínová L, Dráber P, Cifra M. Reversible and irreversible modulation of tubulin self-assembly by intense nanosecond pulsed electric fields. Adv Mater 2019;31:1903636. https://doi.org/10.1002/adma.201903636

[29] Urabe G, Sato T, Nakamura G, Kobashigawa Y, Morioka H, Katsuki S. 1.2 MV/cm pulsed electric fields promote transthyretin aggregate degradation. Sci Rep 2020;10:12003. https://doi.org/10.1038/s41598-020-68681-0⟨http://www.nature.com/articles/s41598-020-68681-0⟩.

[30] Havelka D, Zhernov I, Teplan M, Lánský Z, Chafai DE, Cifra M. Lab-on-chip microscope platform for electro-manipulation of a dense microtubules network. Sci Rep 2022;12:2462. https://doi.org/10.1038/s41598-022-06255-y⟨https://www.nature.com/articles/s41598-022-06255-y⟩.

[31] van den Heuvel MGL, Butcher CT, Lemay SG, Diez S, Dekker C. Electrical docking of microtubules for kinesin-driven motility in nanostructures. Nano Lett 2005;5:235–41. https://doi.org/10.1021/nl048291n

[32] Van den Heuvel MGL, De Graaff MP, Dekker C. Microtubule curvatures under perpendicular electric forces reveal a low persistence length. Proc Natl Acad Sci USA 2008;105:7941–6⟨http://www.pnas.org/content/105/23/7941.short⟩.

[33] Timmons JJ, Preto J, Tuszynski JA, Wong ET. Tubulin's response to external electric fields by molecular dynamics simulations. PLOS One 2018;13:e0202141. https://doi.org/10.1371/journal.pone.0202141

[34] Saeidi HR, Setayandeh SS, Lohrasebi A. Molecular modeling of oscillating GHz electric field influence on the kinesin affinity to microtubule. Chin Phys B 2015;24:080701. https://doi.org/10.1088/1674-1056/24/8/080701⟨http://stacks.iop.org/1674-1056/24/i=8/a=080701?key=crossref.cb55b206152a211a6b1dd1db58ea5872⟩.

[35] Setayandeh SS, Lohrasebi A. Flexibility and kinesin affinity of paclitaxel stabilized microtubule under the influence of GHz electric fields: a molecular modeling approach. J Nanosci Nanotechnol 2018;18:7902–6. https://doi.org/10.1166/jnn.2018.15531

[36] Průša J, Cifra M. Molecular dynamics simulation of the nanosecond pulsed electric field effect on kinesin nanomotor. Sci Rep 2019;9:19721. https://doi.org/10.1038/s41598-019-56052-3⟨http://www.nature.com/articles/s41598-019-56052-3⟩.

[37] Verhey KJ, Kaul N, Soppina V. Kinesin assembly and movement in cells. Annu Rev Biophys 2011;40:267–88. https://doi.org/10.1146/annurev-biophys-042910-155310

[38] Brendza RP, Serbus LR, Duffy JB, Saxton WM. A function for kinesin i in the posterior transport of oskar mRNA and Staufen protein. Science 2000;289:2120–2⟨https://www.ncbi.nlm.nih.gov/pmc/articles/PMC1764218/⟩.

[39] Glater EE, Megeath LJ, Stowers RS, Schwarz TL. Axonal transport of mitochondria requires milton to recruit kinesin heavy chain and is light chain independent. J Cell Biol 2006;173:545–57. https://doi.org/10.1083/jcb.200601067

[40] Palacios IM, Johnston DS. Kinesin light chain-independent function of the Kinesin heavy chain in cytoplasmic streaming and posterior localisation in theDrosophila oocyte. Development 2002;129:5473–85. https://doi.org/10.1242/dev.00119

[41] Jolly AL, Kim H, Srinivasan D, Lakonishok M, Larson AG, Gelfand VI. Kinesin-1 heavy chain mediates microtubule sliding to drive changes in cell shape. Proc Natl Acad Sci USA 2010;107:12151–6. https://doi.org/10.1073/pnas.1004736107

[42] Chakraborty S, Zheng W. Decrypting the structural, dynamic, and energetic basis of a monomeric kinesin interacting with a tubulin dimer in three ATPase states by all-atom molecular dynamics simulation. Biochemistry 2015;54:859–69. https://doi.org/10.1021/bi501056h

[43] Ayoub AT, Klobukowski M, Tuszynski JA. Detailed per-residue energetic analysis explains the driving force for microtubule disassembly. PLOS Comput Biol 2015;11:e1004313. https://doi.org/10.1371/journal.pcbi.1004313

[44] Hub JS, de Groot BL, van der Spoel D. g_wham – a free weighted histogram analysis implementation including robust error and autocorrelation estimates. J Chem Theory Comput 2010;6:3713–20. https://doi.org/10.1021/ct100494z. (publisher: American Chemical Society).

[45] Tyner KM, Kopelman R, Philbert MA. Nanosized voltmeter enables cellular-wide electric field mapping. Biophys J 2007;93:1163–74. https://doi.org/10.1529/biophysj.106.092452⟨http://linkinghub.elsevier.com/retrieve/pii/S0006349507713747⟩.

[46] Slocum JD, Webb LJ. Measuring electric fields in biological matter using the vibrational Stark effect of nitrile probes. Annu Rev Phys Chem 2018;69:253–71.

[47] Isojima H, Iino R, Niitani Y, Noji H, Tomishige M. Direct observation of intermediate states during the stepping motion of kinesin-1. Nat Chem Biol 2016;12:290–7. https://doi.org/10.1038/nchembio.2028

[48] Ramaiya A, Roy B, Bugiel M, Schäffer E. Kinesin rotates unidirectionally and generates torque while walking on microtubules. Proc Natl Acad Sci USA 2017;114:10894–9. https://doi.org/10.1073/pnas.1706985114

[49] Kushwaha VS, Peterman EJG. The temperature dependence of kinesin motor-protein mechanochemistry. Biochem Biophys Res Commun 2020;529:812–8. https://doi.org/10.1016/j.bbrc.2020.06.004⟨https://www.sciencedirect.com/science/article/pii/S0006291×20311980⟩.

[50] Schnitzer MJ, Visscher K, Block SM. Force production by single kinesin motors. Nat Cell Biol 2000;2:718–23. https://doi.org/10.1038/35036345⟨http://www.nature.com/articles/ncb1000_718⟩.
[51] Kuo T-L, Garcia-Manyes S, Li J, Barel I, Lu H, Berne BJ, et al. Probing static disorder in Arrhenius kinetics by single-molecule force spectroscopy. Proc Natl Acad Sci USA 2010;107:11336–40. https://doi.org/10.1073/pnas.1006517107.⟨https://www.pnas.org/content/107/25/11336⟩. (publisher: National Academy of Sciences Section: Biological Sciences).
[52] Zarzycki P, Gilbert B. Temperature-Dependence of the Dielectric Relaxation of Water Using Non-Polarizable Water Models. Phys Chem Chem Phys 2020. https://doi.org/10.1039/C9CP04578C
[53] Martin DR, Friesen AD, Matyushov DV. Electric Field inside a 'Rossky Cavity' in Uniformly Polarized Water. J Chem Phys 2011;135(8):084514.
[54] Kim AJ, Endow SA. A kinesin family tree. J Cell Sci 2000;113:3681–2. https://doi.org/10.1242/jcs.113.21.3681
[55] Hirokawa N, Nitta R, Okada Y. The mechanisms of kinesin motor motility: lessons from the monomeric motor KIF1A. Nat Rev Mol Cell Biol 2009;10:877–84. https://doi.org/10.1038/nrm2807⟨http://www.nature.com/articles/nrm2807⟩.
[56] Schimert KI, Budaitis BG, Reinemann DN, Lang MJ, Verhey KJ. Intracellular cargo transport by single-headed kinesin motors. Proc Natl Acad Sci USA 2019;116:6152–61. https://doi.org/10.1073/pnas.1817924116. (publisher: Proceedings of the National Academy of Sciences).
[57] Andreasson JO, Milic B, Chen G-Y, Guydosh NR, Hancock WO, Block SM. Examining kinesin processivity within a general gating framework. eLife 2015;4:e07403. https://doi.org/10.7554/eLife.07403. (publisher: eLife Sciences Publications, Ltd).
[58] Kühn S, Liu Q, Eing C, Frey W, Nick P. Nanosecond electric pulses affect a plant-specific kinesin at the plasma membrane. J Membr Biol 2013;246:927–38. https://doi.org/10.1007/s00232-013-9594-z
[59] Uchimura S, Oguchi Y, Katsuki M, Usui T, Osada H, Nikawa J-i, et al. Identification of a strong binding site for kinesin on the microtubule using mutant analysis of tubulin. EMBO J 2006;25:5932–41. https://doi.org/10.1038/sj.emboj.7601442⟨https://www.ncbi.nlm.nih.gov/pmc/articles/PMC1698889/⟩.
[60] Braun M, Lansky Z, Szuba A, Schwarz FW, Mitra A, Gao M, et al. Changes in microtubule overlap length regulate kinesin-14-driven microtubule sliding. Nat Chem Biol 2017;13:1245. https://doi.org/10.1038/nchembio.2495
[61] Bujak Ł, Holanová K, García Marín A, Henrichs V, Barvík I, Braun M, et al. Fast leaps between millisecond confinements govern Ase1 diffusion along microtubules. Small Methods 2021;5:2100370. https://doi.org/10.1002/smtd.202100370
[62] Mickolajczyk KJ, Deffenbaugh NC, OrtegaArroyo J, Andrecka J, Kukura P, Hancock WO. Kinetics of nucleotide-dependent structural transitions in the kinesin-1 hydrolysis cycle. Proc Natl Acad Sci USA 2015;112:E7186–93. https://doi.org/10.1073/pnas.1517638112
[63] Vala M, Bujak Ł, García Marín A, Holanová K, Henrichs V, Braun M, et al. Nanoscopic structural fluctuations of disassembling microtubules revealed by label-free super-resolution microscopy. Small Methods 2021;5:2000985. https://doi.org/10.1002/smtd.202000985
[64] Robert HML, Holanová K, Bujak Ł, Vala M, Henrichs V, Lánský Z, et al. Fast photothermal spatial light modulation for quantitative phase imaging at the nanoscale. Nat Commun 2021;12:2921. https://doi.org/10.1038/s41467-021-23252-3.⟨https://www.nature.com/articles/s41467-021-23252-3⟩. number: 1 Publisher: Nature Publishing Group.
[65] Havelka D, Chafai DE, Krivosudský O, Klebanovych A, Vostárek F, Kubínová L, et al. Nanosecond pulsed electric field lab-on-chip integrated in super-resolution microscope for cytoskeleton imaging. Adv Mater Technol 2020;5:1900669. https://doi.org/10.1002/admt.201900669